Die Deutsche Bibliothek - CIP-Einheitsaufnahme

7. Internationales Aachener Schweißtechnik Kolloquium: Hochleistungsfügeverfahren: Grundlagen, Anwendungen, Ausrüstungen; High Productivity Joining Processes: Fundamentals, Applications, Equipment (Band II)/ Ulrich Dilthey (Hrsg.).
Aachen : Shaker, 2001
(Aachener Berichte Fügetechnik)
ISBN 3-8265-8759-6

Printed in Germany.

ISBN 3-8265-8759-6
ISSN 0943-9358

Shaker Verlag GmbH • P.O. BOX 1290 • D-52013 Aachen
Phone: 0049/2407 /9596-0 • Telefax: 0049/2407/9596-9
Internet: www.shaker.de • eMail: info@shaker.de

Estimation of Microstructure in Steel Welds

Beurteilung des Mikrogefüges von Stahlschweißnähten

H. K. D. H. Bhadeshia

Department of Materials Science and Metallurgy, University of Cambridge/United Kingdom

Kurzzusammenfassung

Physikalische Modelle zur Entwicklung von Mikrostrukturen haben das Potential, neue Phänomene und Eigenschaften zu enthüllen. Sie können auch dazu beitragen, beeinflussende Variablen zu identifizieren. Die Möglichkeit, die Mikrostruktur unter allen Umständen abschätzen zu können, ist zu einem großen Teil vom Verständnis der Mechanismen von Festkörperumwandlungen abhängig. Sobald dieses Verständnis erreicht ist, kann eine Reihe von Näherungen zur quantitativen Beschreibung der Vorgänge beim Erstarren und Abkühlen des Schmelzbades auf Umgebungstemperatur benutzt werden. Dieser Beitrag faßt die heute verfügbaren Methoden zu Vorhersage der sich im Schweißgut ausbildenden Mikrostruktur ferritischer Stählen zusammen, die in Ingenieurbauten, wie Brücken oder Schffen, verarbeitet werden.

Introduction

It is often said that a welded joint contains features typical of all aspects of physical metallurgy. This especially true of the ferritic steels used in engineering constructions. The general weld problem is illustrated in Figure 1. It summarises the ultimate goal and gives an indication of the task that lies ahead. Although the complexity of the problem can be daunting, good solutions can be achieved. A number of reviews have been compiled on the subject of this paper /1, 2/; detailed references, which are omitted here for brevity, can be found in those review articles. The purpose of this paper is to present the essence of the approximations used in the numerical prediction of solid-state transformations in welds.

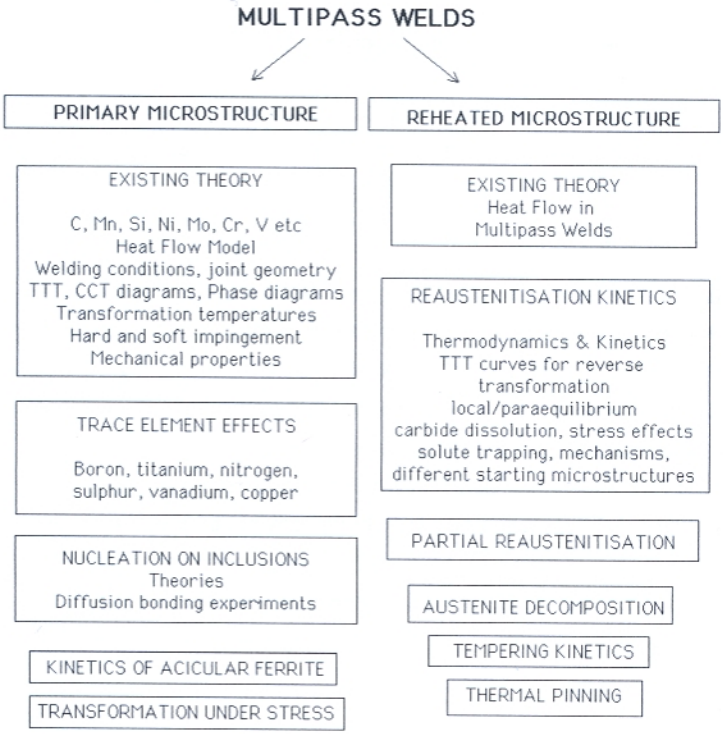

Figure 1: Chart showing the components of weld microstructure evolution models
Bild 1: Diagramm mit Komponenten von Evolutionsmodellen zur Bestimmung der Mikrostruktur im Schweißgut

The Austenite Grain Structure

Most weld deposits for structural steels begin solidification with the epitaxial growth of delta-ferrite (δ) from the hot grain-structure of the parent plate at the fusion surface. The large temperature gradients at the solid/liquid interface ensure that solidification proceeds with a cellular front; final δ-grains are therefore columnar in shape. The major axes of the grains tend to lie along the direction of maximum heat flow whenever their crystallographic orientation permits. On further cooling, austenite allotriomorphs nucleate at the δ-ferrite grain boundaries and their higher rate of growth along the δ-δ boundaries (and presumably also the temperature gradients) leads to the formation of columnar austenite grains whose

shape resembles that of the original solidification structure. Since welding involves a moving heat source, the orientation of the temperature isotherms alters with time. Consequently, the major growth direction of the austenite is found to be somewhat different from that of the δ-grains.

Both the shape and size of the austenite grains is of importance in the evolution of the final microstructure. The effect of the austenite grain size is two fold: there is firstly the usual phenomenon in which the number density of austenite grain boundary heterogeneous nucleation sites increases with the total grain boundary area per unit volume of sample. This amounts to the classical and well established hardenability variation with austenite grain size. The second, and more subtle effect, arises from the grain-shape anisotropy. Although the columnar grains of austenite are very long, the evolution of many aspects of the microstructure within an individual austenite grain is dependent on the mean lineal intercept within that grain. Since the chances of test lines lying parallel to the longest dimension of the columnar grain are small, the mean lineal intercept depends mainly on the width of the grain. As will be seen later, this means that the grain length can often be excluded as a factor in the calculation of microstructure.

The anisotropy of grain structure causes certain complications in representing the grain parameters in any microstructure model. The morphology can be described approximately by a uniform, space-filling array of hexagonal prisms. An approximation is that the elongated austenite grains curve as they grow into the weld pool, in response to the changing orientations of the isotherms. The actual grains are also not of uniform size. Each hexagonal prism can be represented by its length c and cross-sectional side length a. With these approximations, the mean lineal intercept $\underline{L}$ and mean areal intercept $\underline{A}$, as measured from several *differently oriented sections* are given by:

$$\underline{L} = \sqrt{12}ac/\left(\sqrt{3}a + 2c\right) \equiv \sqrt{3}a \tag{1}$$

$$\underline{A} = \sqrt{27}a^2c/(3a + c) \equiv \sqrt{27}a^2 \tag{2}$$

the approximations being valid when, as is generally the case for weld deposits. By measuring these quantities, the parameters c and can be determined. This is unfortunately, difficult to do, and is not completely necessary for microstructure modelling if some further reasonable approximations are made. The most important parameter is the quantity a if $c \gg a$. The men lineal intercept measured at random on a longitudinal section (which reveals equiaxed austenite grain sections) of the weld, is given by

$$\underline{L}_t = \pi a \cos\{30°\}/2 \tag{3}$$

On the other hand, it has been common practice to define the austenite grain size from the transverse section of a weld, with the size being measured not at random, but by aligning the test lines normal to the larger dimension of the grain sections. If it is assumed that the *c*-axes of the austenite grains lie in the plane of the transverse section, then the mean lineal intercept $\underline{L}_{tn}$ measured in the traverse section in a direction normal to the major axes of the grain sections turns out to be identical to $\underline{L}_t$, and is relatively easy quantity to measure.

Factors Influencing Size

It is not possible as yet to predict the austenite grain size (e. g. $\underline{L}_{tn}$) of steel welds; even the factors controlling this grain size are far from clear. It has naturally been assumed, by extrapolation from grain growth theory, that the nonmetallic inclusions which are common in steel welds control the grain size by Zener pinning the boundaries. This analogy is doubtful since the austenite grains form by the transformation of δ-ferrite, whereas Zener pinning deals with the hindrance of grain boundaries during grain growth. The driving force for grain growth typically amounts to just a few Joules per mole, whereas that for transformation from δ-ferrite to austenite increases indefinitely with undercooling below the equilibrium transformation temperature. Pinning of δ/γ interfaces cannot then be effective, unless the grain structure coarsens after transformation is completed. The columnar austenite grain size must to some extent correlate with the grain size in the parent plate at the fusion boundary, since solidification occurs by the epitaxial growth of those grains. However, the relationship cannot be simple, since during solidification, those grains with their < 1 0 0 > directions most parallel to the direction of steepest temperature gradient grow rapidly, stifling the grains which are not suitably oriented. Consequently, the crystallographic texture of the parent plate, and the plane of that plate on which the weld is deposited, must influence the final austenite grain structure. Clear differences in the austenite grain structure were found between three welds deposited on mutually perpendicular faces of the same sample, in a recent experiment designed to illustrate the influence of crystallographic texture on the grain size. Moresystematic work is now called for. A corollary is that particles in the parent plate (e. g. carbo-nitrides) may limit the coarsening of the plate grains at the fusion boundary, and therefore lead ultimately to a smaller grain size in the fusion zone.

Regression equations are currently used in making crude estimates of the columnar austenite grain size as a function of chemistry and heat input. If these are to believed, then the alloy chemistry itself has a significant effect on grain structure, perhaps by influencing the thermodynamics and kinetics of the $\delta \rightarrow \gamma$ transformation.

As-Deposited Primary Microstructure

The microstructure obtained as the weld cools from the liquid phase to ambient temperature is called the *as-deposited* or *primary* microstructure. It consists of allotriomorphic ferrite α, Widmanstätten ferrite α_w, acicular ferrite α_a, and the so-called microphases, which might include small amounts of martensite, retained austenite or degenerate pearlite, Figure 2. Bainite consisting of sheaves of parallel platelets is also found in some weld deposits, particularly of the type used in the power generation industry.

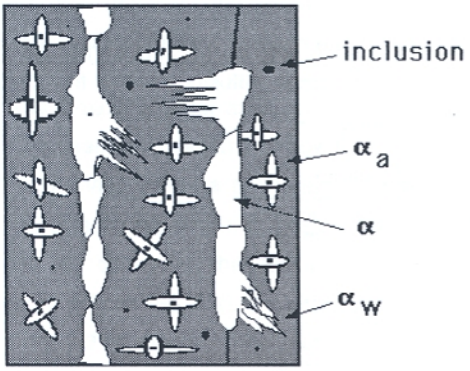

Figure 2: The essential constituents of the primary microstructure in the columnar austenite grains of a steel weld deposit

Bild 2: Die wesentlichen Bestandteile der primären Mikrostruktur säulenförmiger Austenitkörner einer Stahl-Auftragschweis-sung

The above description is incomplete for multirun welds, in which some of the regions of original primary microstructure are reheated to temperatures high enough to cause reverse transformation into austenite, which during the cooling part of the thermal cycle retransforms into a different microstructure. Other regions may simply be tempered by the deposition of subsequent runs. The microstructure of the reheated regions is called the *reheated* or *secondary* microstructure.

Allotriomorphic ferrite

Allotriomorphic ferrite (α) is the first phase to form on cooling below the A_{e3} temperature and nucleates heterogeneously at the boundaries of the columnar austenite grains. Original references to details of allotriomorphic ferrite formation have been presented elsewhere /1, 2/.

In low alloy steel welds, the boundaries rapidly become decorated with continuous layers of ferrite, so that subsequent transformation simply involves the reconstructive thickening of these layers, a process which can be modelled in terms of the normal migration of planar α/γ interfaces. If it is assumed that the growth of allotriomorphic ferrite occurs under paraequilibrium conditions, then the half-thickness q of the layer during isothermal growth is given by:

$$q = \alpha_1 t^{1/2} \tag{4}$$

where α_1 is the one-dimensional parabolic tickening rate constant, and t is the time defined to begin from the initiation of growth. The parabolic relation implies that the growth rate slows down as the ferrite grows as the carbon diffusion field in the austenite gets bigger with the thickness of the ferrite, Figure 3.

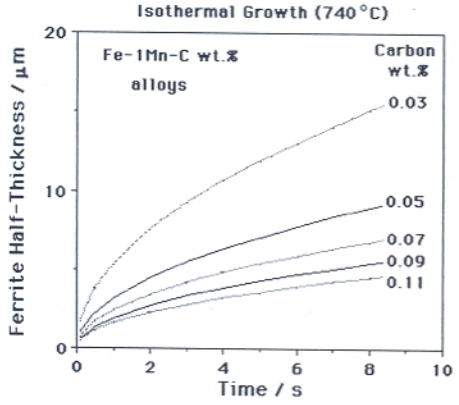

Figure 3: Diagram illustrating how the calculated thickness of an allotriomorphic ferrite layer increases during isothermal transformation, in the absence of soft-impingement effects. Each curve represents a Fe-1Mn-C wt.% steel with the carbon concentration as indicated on the diagram

Bild 3: Diagramm zur Darstellung der Dickenzunahme einer allotrimorphen ferritischen Schicht während der isothermischen Transformation bei Fehlen weicher Stoßeffekte. Jede Kurve repräsentiert einen Fe-1Mn-C wt.% Stahl mit dem jeweils im Diagramm dargestellten Kohlenstoffgehalt.

Paraequilibrium is a constrained equilibrium in which the ratio of iron to substitutional solute concentration remains constant everywhere, but subject to that constraint, the carbon achieves equality of chemical potential. It seems a reasonable assumption given that welds generally cool at a rapid rate. The parabolic rate constant is obtained by solving the equation:

$$2\sqrt{\frac{\underline{D}}{\pi}}\frac{x^{\gamma\alpha}-\bar{x}}{x^{\gamma\alpha}-x^{\alpha\gamma}}=\alpha_1\exp\left\{\frac{\alpha_1^2}{4\underline{D}}\right\}\mathrm{erfc}\left\{\frac{\alpha_1}{2\sqrt{\underline{D}}}\right\}$$

where $x^{\gamma\alpha}$ and $x^{\alpha\gamma}$ are at the paraequilibrium carbon concentrations in austenite and ferrite respectively at the interface (obtained using a calculated multicomponent phase diagram), $\bar{x}$ is the average carbon concentration inthe alloy and $\underline{D}$ is a weighted average diffusivity of carbon in austenite, given by:

$$\underline{D}=\int_{x^{\gamma\alpha}}^{\bar{x}}\frac{D\{x\}dx}{\bar{x}-x^{\gamma\alpha}}$$

where D is the diffusivity of carbon in austenite at a particular concentration of carbon.

In welds transformations occur during cooling to ambient temperature, whereas the above discussion focuses on isothermal growth. This can be remedied by integrating the thickening of the layers over a temperature range T_h to T_l. Allotriomorphic ferrite growth begins at T_h, a temperature which can be estimated using a calculated TTT curve, and Scheil's rule to allow for the fact that the process involves continuous cooling transformation. It "finishes" at T_l, the temperature where the reconstructive and displacive C-curves of the TTT diagram intersect (i. e. where displacive transformations have a kinetic advantage). Thus

$$q=\int_{t=0}^{t_l}0.5\alpha_1 t^{-0.5}+\frac{\alpha_1}{t}t^{0.5}\quad dt \tag{5}$$

where $t = 0$ at T_h and $t = t_l$ at T_l. The second term on the right hand side of this expression has been neglected in previous analyses - its significance has yet to be determined.

The volume fraction of ferrite is given by

$$v_a=[2q\tan\{30°\}(2a-2q\tan\{30°\})]/a^2 \tag{6}$$

so that the dependence on austenite grain size becomes obvious. This equation is found to represent the volume fraction of allotriomorphic ferrite extremely well, but only after an

empirical correction by a factor of about 2 - the fraction is always underestimated.

Effect of Solidification - Induced Segregation

There are two major causes of chemical segregation in welds, the relatively large cooling rates involved and variations in process parameters during welding. The latter cannot in general be accurately predicted, but the extent of segregation due to nonequilibrium solidification can be estimated from the partition coefficient k_i which is the ratio of the concentration of element i in the δ-ferrite to that in the liquid phase. The coefficient can be calculated for the liquidus temperature, and the minimum concentration to be found in a heterogeneous solid weld is then taken to be $k_i \bar{x}$. This is the composition of the solute-depleted region of the weld, since it is assumed that diffusion during cooling to ambient temperatures does not lead to significant homogenisation. Carbon, which diffuses much more rapidly than substitutional solutes, is assumed to be homogeneously distributed in the austenite prior to transformation.

The method for incorporating the effect of substitutional solute segregation into weld microstructure calculations, is via the influence on the temperature at which the allotriomorphic ferrite begins to grow (T_h). In general, it is the solute depleted regions which should transform first to ferrite. Thus, the TTT diagram used for estimating T_h should be calculated not from the average composition of the steel, but using the composition of the solute depleted regions.

This procedure seems to work well, presumably because the major effect of substitutional solute segregation during the welding of low-alloy steels is on enhancing the nucleation of allotriomorphic ferrite, and hence on the temperature range $T_h \rightarrow T_l$. The effect of chemical segregation becomes more pronounced as the level of alloying additions rises.

Widmanstätten Ferrite

The lengthening rate G of Widmanstätten ferrite can be estimated using the Trivedi theory for the paraequilibrium diffusion-controlled growth of parabolic cylinders, taking into account the strain energy associated with the transformation mechanism. Because of its shape, and unlike allotriomorphic ferrite, Widmanstätten ferrite grows at a constant rate as long as soft-impingement (overlap of diffusion fields) does not occur. The calculated growth rates are found to be so large for typical weld deposits, that the formation of Widmanstätten ferrite is usually complete within a fraction of a second. Hence, for all

practical purposes, the transformation can be treated as being isothermal.

Transformation to Widmanstätten ferrite is taken to begin when that of allotriomorphic ferrite ceases at T_i; the volume fraction is given by

$$v_w = C_4 G(2a - 4q\tan\{30°\})t_2^2/(2a)^2 \quad (7)$$

where C_4 is a constant independent of alloy composition and t_2 is the time *available* for the formation of Widmanstätten ferrite. Note that the v_W depends not only on the austenite grain size but also on the thickness of the layer of allotriomorphic ferrite which formed earlier. In fact the situation is more complex, as indicated by the fact that v_W hardly correlates with G. Hard impingement with intragranularly nucleated acicular ferrite has to be taken into account, Figure 4; this depends on the time t_c, which is the time between the cessation of allotriomorphic ferrite and the onset of acicular ferrite. if the time interval $t_3 = (2a\sin\{60°\} - 2q) / G$ required for an α_ω plate to grow unhindered across the austenite grain is less than t_c, α_ω plates can grow unhindered across the austenite grain (i. e. $t_2 = t_3$), but if not, then $t_2 = t_c$. When an algorithm is included to account for all this, the calculated volume fraction v_W is found to be in good agreement with experiments.

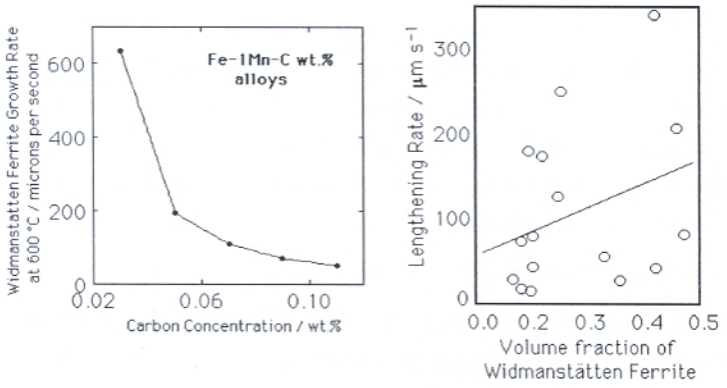

Figure 4: (a) The calculated isothermal growth rates of Widmanstätten ferrite in a series of Fe-alloys as a function of carbon concentration. Notice that the growth rates are so large, that the plates could grow right across typical austenite grains within a fraction of a second. (b) Poor correlation of the volume fraction of Widmannstätten ferrite against the calculated growth rate

Bild 4: (a) Berechnete isothermische Wachstumsraten von Widmanstätten Ferrit in einer Reihe von 1Mn-C wt.% Legierungen als Funktion der Kohlenstoffkonzentration. Anzumerken ist, daß die Wachstumsraten so groß sind, daß die Lamellen die typische Austenitkorngröße inerhalb eines Bruchteils einer Sekunde überschreiten könnten. (b) Schlechte Übereinstimmung zwischen Volumenanteil von Widman-stätten Ferrit und berechneter Wachstumsrate

Acicular Ferrite

It is now clear that "acicularferrite" α_a is essentially intragranularly nucleated bainite, the heterogeneous nucleation sites being complex nonmetallic inclusions. The classic work by Ito, Nakanishi and Komizo demonstrated that it forms below the bainite-start temperature. Some of the other similarities and facts which support the identity of bainite and acicular ferrite are:

1. They both exhibit the invariant-plane strain shape deformations with large shear components, during growth. Consequently, the growth of a plate of acicular ferrite or bainite is confined to a single austenite grain (i. e. it is hindered by a grain boundary) since the coordinated movement of atoms implied by the shape change cannot in general be sustained across a border between grains in different crystallographic orientations. A further implication is that plates of acicular ferrite, like bainite, *always* have an orientation relationship with the parent phase, which is within the Bain region. This is not necessarily the case when the transformation occurs by a reconstructive mechanism.
2. There is no substitutional solute partitioning during the growth of either bainite or acicular ferrite.
3. Both reactions stop when the austenite carbon concentration reaches a value where it becomes thermodynamically impossible to achieve diffusionless growth. Any redistribution of carbon from the supersaturated ferrite plates occurs after growth. Growth is thus diffusionless, but is followed immediately afterwards by the recection of carbon into the residual austenite.
4. Acicular ferrite only forms below the bainite-start temperature.
5. There is a large and predictable hysteresis in the temperature at which austenite formation begins from a mixed microstructure of acicular ferrite and austenite, or bainite and austenite.
6. The removal of inclusions from a weld deposit, without changing any other feature, causes a change in the microstructure from acicular ferrite to bainite.
7. An increase in the number density of austenite grain surface nucleation sites (relative to intragranular sites) causes a transition from acicular ferrite to bainite.
8. The elimination of austenite grain surfaces by decoration with inert allotriomorphic ferrite leads to a transition from a bainitic to an acicular ferritic microstructure.

Although there is a lot of work in progress, there are as yet no models which allow the volume fraction v_α of acicular ferrite to be calculated from first principles. For many welds it is nevertheless possible to estimate v_α via the equation

$$v_a = 1 - v_\alpha - v_W - v_m \tag{8}$$

where v_m is the volume fraction of microphases.

The development of a reliable model for acicular ferrite depends on an understanding of its mechanism of transformation, and of the role of inclusions as nucleation sites, as has been emphasised elsewhere. The detailed appearance of acicular ferrite is different from that of conventional bainite because the former nucleates intragranularly at inclusions within large γ grains whereas in wrought steels which are relatively free of nonmetallic inclusions, bainite nucleates initially at γ / γ grain surfaces and continues growth by the repeated formation of subunits, to generate the classical sheaf morphology. Acicular ferrite does not normally grow in sheaves because the development of sheaves is stifled by hard impingement between plates nucleated independently at adjacent sites. Indeed, conventional bainite or acicular ferrite can be obtained under identical isothermal transformation conditions in the same (inclusion rich) steel. In the former case, the austenite grain size has to be small in order that nucleation from grain surfaces dominates and subsequent growth then swamps the interiors of the austenite grains. For a larger austenite grain size, intragranular nucleation on inclusions dominates, so that acicular ferrite is obtained, Figure 5. Hence, the reason why acicular ferrite is not usually obtained in wrought steels is because they are relatively free of inclusions and because most commercial heat treatments aim at a small austenite grain size.

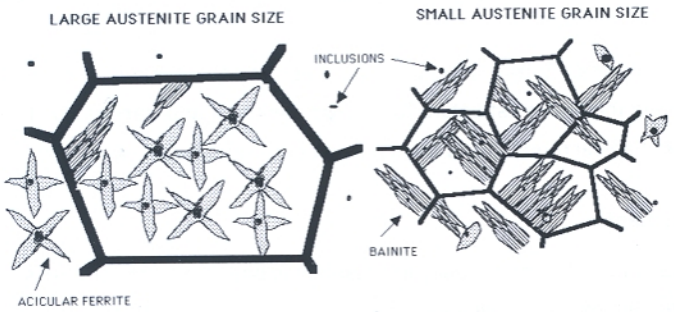

Figure 5: The effect of austenite grain size in determining whether the microstructure is predominantly acicular ferrite or bainite

Bild 5: Der Einfluß der Austenitkorngröße auf die Bestimmung, ob das Gefüge vorherrschend acicular ferritisch oder bainitisch ausgebildet ist

Some example calculations of weld metal microstructure are presented in Figure 6; predictions like these have been extensively validated using published experimental data and by designing new experiments.

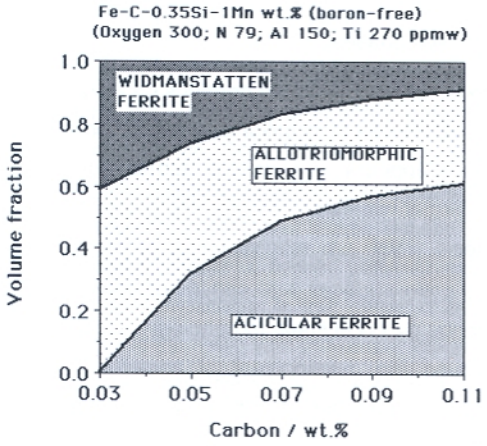

Figure 6: An example of microstructure calculations
Bild 6: Ein Beispiel für berechnete Mikrostrukturen

Summary

There is little doubt that welding metallurgy remains one of the exhilarating topics of materials science. In this paper we have described one small aspect of welding metallurgy, the calculation of weld metal microstructure for structural steels used at ambient or subzero temperatures. Similar progress has been made in many other areas in the modelling of weld metal microstructure for a large variety of applications /3/. The modelling of complex mechanical properties is another area of major interest /4/.

Acknowledgement

It is a pleasure to have this opportunity to present this paper in honour Professor U. Dilthey who has made seminal contributions to the understanding of welding, both in science and technology.

References

/1/ H. K. D. H. Bhadeshia and L.-E. Svensson:

Mathematical Modelling of Weld Phenomena, eds H. Cerjak and K. E. Easterling, Institute of Materials, London, (1993) 109-182.

/2/ O. Grong:

Metallurgical Modelling of Welding, 2nd edition, Institute of Materials, London (1997) 1-602.

/3/ H. K. D. H. Bhadeshia:

Trends in Welding Research, eds S. A. David, T. DebRoy, J. A. Johnson, H. B. Smartt and J. M. Vitek, ASM International Ohio, (1999) 795-804.

/4/ H. K. D. H. Bhadeshia and L.-E. Svensson:

Mathematical Modelling of Weld Phenomena III, eds H. Cerjak and H. K. D. H. Bhadeshia, Institute of Materials, London, (1997) 229-284.

Hochleistungsfügeverfahren
Grundlagen, Anwendungen, Ausrüstungen

High Productivity Joining Processes
Fundamentals, Applications, Equipment

Band II
Volume II

ASTK'01
7. Internationales Aachener Schweisstechnik Kolloquium
Eurogress Aachen, 03. - 04. Mai 2001
7th International Aachen Welding Conference
Eurogress Aachen, 3rd - 4th May, 2001